

# Self-Lensing Models of the LMC

G. Gyuk, N. Dalal, & K. Griest

*Physics Department, University of California, San Diego, CA 92093*

July 23, 1999

## ABSTRACT

All of the proposed explanations for the microlensing events observed towards the LMC have difficulties. One of these proposed explanations, LMC self-lensing, which invokes ordinary LMC stars as the long sought-after lenses, has recently gained considerable popularity as a possible solution to the microlensing conundrum. In this paper, we carefully examine the set of LMC self-lensing models. In particular, we review the pertinent observations made of the LMC, and show how these observations place limits on such self-lensing models. We find that, given current observational constraints, *no* purely LMC disk models are capable of producing optical depths as large as that reported in the MACHO collaboration 2-year analysis. Besides pure disk, we also consider alternate geometries, and present a framework which encompasses the previous studies of LMC self-lensing. We discuss which model parameters need to be pushed in order for such models to succeed. For example, like previous workers, we find that an LMC halo geometry may be able to explain the observed events. However, since *all* known LMC tracer stellar populations exhibit disk-like kinematics, such models will have difficulty being reconciled with observations. For SMC self-lensing, we find predicted optical depths differing from previous results, but more than sufficient to explain all observed SMC microlensing. In contrast, for the LMC we find a self-lensing optical depth contribution between  $0.47 \cdot 10^{-8}$  and  $7.84 \cdot 10^{-8}$ , with  $2.44 \cdot 10^{-8}$  being the value for the set of LMC parameters most consistent with current observations.

*Subject headings:* microlensing, dark matter, MACHOs, Magellanic Clouds, galaxies: (halos, kinematics, dynamics)

## 1. Introduction

Gravitational microlensing has become a powerful tool for the discovery, limiting, and characterization of populations of dark (and luminous) objects in the vicinity of the Milky Way. Of great interest is the interpretation of the handful of events discovered towards the Magellanic Clouds. If these events are due to a population of objects in an extended Milky Way halo, they can be interpreted to represent between 20% and 100% of the dark matter in our Galaxy (Alcock, et al. 1997a; Gates, Gyuk, & Turner 1996). However, the most probable masses of these objects lie in the 0.1 to  $1M_{\odot}$  mass range (Alcock, et al. 1997a). Such a large number of objects in this mass range is quite problematic (e.g. Fields, et al. 1998). Therefore alternatives to MW halo lensing have been sought to explain the LMC microlensing events.

One alternative, first proposed by Sahu (1994a), suggests that stars within the LMC itself, lensing other LMC stars, could produce the observed optical depth. This claim has been disputed by several other groups (Gould, 1995; Alcock, et al. 1997a), who claim that the rate of LMC self-lensing is far too low to account for the observed rate. It was hoped that observation along a different line of sight (i.e. towards the SMC) would resolve this issue. After 5 years of monitoring, there have been two observed microlensing events towards the SMC. The more recent SMC event was a resolved binary lens event (Alcock, et al. 1998), allowing determination of the lens distance (Alcock, et al. 1998; Afonso, et al. 1998; Albrow, et al. 1998). The lens was found to lie, with high probability, in the SMC and not in the Milky Way halo. There is also evidence that the only other SMC microlensing event (Alcock, et al. 1997c) may reside in the SMC (Palanque-Delabrouille, et al. 1998). Thus all of the relevant lenses whose distances are known are thought to reside in the Magellanic Clouds. This has been interpreted by some as settling the case in favor of the LMC/LMC self lensing interpretation of the LMC events. This conclusion is not well-founded if based solely on the SMC events. The reason, as we discuss below, is fairly simple – the SMC is known to be extended along the line-of-sight, while there is little evidence that the LMC is similarly extended. In fact, the observations imply that the LMC is distributed as a thin disk, quite unlike its smaller sibling. Thus, unfortunately, the SMC microlensing events do not

settle the question of the interpretation of the LMC events, and the controversy remains.

The purpose of this paper is to provide a set of calculations of LMC microlensing that treats LMC self-lensing in a systematic, thorough fashion. We relate the known LMC observations to microlensing predictions, and provide a framework in which future observations will easily translate into microlensing predictions. We hope this will serve as a general basis for comparison between observation and theory in the future.

Overall, we find that self lensing models typically suffer two major defects. First, it is quite difficult for such models to produce enough lensing to account for the observed optical depth, while remaining within the bounds set by observation. Second, the optical depth due to disk or bar self-lensing is strongly concentrated on the sky, in contrast to the rather uniform distribution of events seen to date. These two statements have a major caveat: if the LMC lenses are distributed in an extended or halo-like geometry, it is possible to produce the required optical depth, and the central concentration of the predicted events is significantly diminished. Such an extended or halo-like distribution, however, requires either an hitherto undetected stellar population, or a dark MACHO component to the LMC halo. If a dark LMC halo is invoked, then one might expect it to have a similar fraction of dark MACHOs as the Milky Way Halo. Otherwise, the presence of such a component in the LMC but not in the Galactic halo would be puzzling. On the other hand, if a stellar LMC halo with a luminosity function similar to the disk is invoked, direct observation of these LMC halo stars should be possible. Indeed, as we review below, several stellar populations which correspond to stars that do trace the spheroid in our Galaxy have been observed in the LMC, and *all* of them fail to exhibit a halo geometry. Therefore, current observations suggest that the number of stars in any such stellar halo is small, and that an LMC stellar halo probably does not greatly contribute to microlensing.

## 2. Microlensing

The first and main reason that previous work has produced such discordant results is that different papers have treated the LMC differently. For example, Gould (1995) and Alcock et al. (1997) treated the LMC as a thin exponential disk, while Sahu (1994a)

and Aubourg et al. (1999) modeled the LMC as being much more extended along the line of sight. These two qualitatively different prescriptions give wildly different predictions for the optical depth and rate of self-lensing. The reason for this is simple. The rate of microlensing is proportional to the Einstein radius of the lenses, which is given by

$$R_E = \left[ 2R_S \frac{D_{OL} D_{LS}}{D_{OS}} \right]^{1/2}$$

where  $R_S$  is the Schwarzschild radius of the lens,  $D_{OL}$  is the angular diameter distance between the observer and lens,  $D_{LS}$  is the distance between the lens and source, and  $D_{OS}$  is the distance between observer and source. The Einstein radius (and thus the microlensing rate) tends to zero as the lens and source approach each other. In the language of Griest (1991), the ‘‘Einstein tube’’ pinches off at the ends. Therefore, if the lenses are confined to a thin plane along with the sources, the microlensing rate must be small. On the other hand, if the lenses are allowed to move away from the sources, the rate increases. This principle is clearly demonstrated in the SMC. Due to its interactions with the LMC and the MW, the SMC is being tidally disrupted and is consequently quite elongated along the line of sight to the MW (Caldwell & Coulson 1986; Welch, *et al.* 1987). This allows stars within the SMC to be along the same line of sight to us, but separated from each other. Consequently, we expect appreciable self-lensing within the SMC, and this expectation is borne out by the large observed SMC self-lensing rate (Alcock, et al. 1997c; Palanque-Delabrouille, et al. 1998). Indeed, EROS 2 reports an observed SMC optical depth of  $\sim 3.3 \cdot 10^{-7}$  (Palanque-Delabrouille, et al. 1998), and employing the simple model Palanque-Delabrouille et al. use to describe the SMC disk, we find predicted self-lensing optical depths of 1.5, 3.0, and  $4.4 \cdot 10^{-7}$  for SMC vertical scale heights of 2.5, 5.0, and 7.5 kpc respectively. (We note that these numbers do not agree with the predicted optical depths that Palanque-Delabrouille et al. report, but we are confident that our values are correct.)

To answer the question of whether LMC self-lensing is significant, we must understand the distribution of stars within the LMC. If the LMC is a thin disk, then the small rates and optical depths derived by Gould and others will be valid. Conversely, if the LMC is puffy, then the large rates and optical depths claimed by Sahu and others will be correct. The basis

for any description of the LMC is the set of observations that have been made of the LMC. We therefore turn to the current state of observations of the LMC.

### 3. Observations and Models of the LMC

#### 3.1. LMC disk

Since the pioneering work of de Vaucouleurs (1957), it has been well accepted that the stellar component of the LMC has an exponential profile. The value de Vaucouleurs measured for the exponential scale length,  $R_d$ , continues to agree with the current value of  $1.8^\circ$  (Alves, et al. 1999), which corresponds to a physical scale length of 1.6 kpc for a distance to the LMC of 50 kpc. In addition to this stellar population, the LMC possesses significant quantities of HI gas, which has recently been mapped out by Kim et al. (1998). Their images show clear spiral structure in the gas, supporting the notion that the LMC is a typical dwarf spiral galaxy. The gas is confined to a thin disk, inclined at roughly  $30^\circ$ , with a position angle  $\sim 170^\circ$ . See Westerlund (1998, p. 30) for a compilation of various estimates of the LMC orientation, as well as Kim et al. (1998) for a recent value. Based on these observations, in this paper we describe the stellar disk by a double exponential profile, given by

$$\rho_d = \frac{M_{disk}}{4\pi z_d R_d^2} e^{-\frac{R}{R_d} - \left| \frac{z}{z_d} \right|},$$

where  $R_d$  is the radial scale length,  $z_d$  is the vertical scale height, and  $M_{disk}$  is the disk mass. Note that  $R_d$  is well constrained by observation, but we have some leeway in the scale height and in the mass of the disk. We discuss these two quantities in more detail later. The disk is inclined at angle  $i$  to our line of sight and has position angle PA.

#### 3.2. LMC Bar

As is well known, the LMC hosts a prominent bar, of size roughly  $3^\circ \times 1^\circ$ . The bar has the unusual (although not unique, e.g. Freeman 1996, Odewahn 1996) property of being offset from the dynamical center of the HI gas. The offset is  $\approx 1.2^\circ$  (Westerlund, 1997), corresponding to a physical offset of  $\sim 1$  kpc. The kinematics of the LMC bar are consistent with solid body rotation (Odewahn 1996), as is seen in numerous barred galaxies. The distribution of matter within the bar is not well known. Measurements of the luminosity function, after subtraction of disk

light, show it to be consistent with an exponential profile along the major axis (Bothun & Thompson 1988; Odewahn 1996). This is consistent with certain other bars, which can be well described by an exponential along the major axis and a Gaussian profile along the minor axis (Blackman 1983; Ohta 1996). For our own Galactic bar, Dwek, et al. (1995) have proposed a profile similar to a Gaussian, but more boxy, and this form is also consistent with bars in certain other galaxies.

Thus, unlike the disk, the bar is not particularly well defined. With little guidance from observations, we have treated the bar simply as a triaxial gaussian, with axis ratios chosen to match the observed ratios. We let

$$\rho_b = \frac{M_{bar}}{(2\pi)^{3/2}x_b y_b z_b} e^{-\frac{1}{2}[(\frac{x}{x_b})^2 + (\frac{y}{y_b})^2 + (\frac{z}{z_b})^2]},$$

where  $x, y, z$  are coordinates along the principal axes of the bar, and  $x_b, y_b, z_b$  are the scale lengths along the three axes.  $M_{bar}$  is the total mass of the bar. This form is somewhat similar to models used to describe other galactic bars, e.g. (Dwek, et al. 1995). We place the bar in the same plane as the disk, however we place the bar center at the position of the observed bar centroid, at ( $\alpha = 5h24m, \delta = -69^\circ 48'$ ) (de Vaucouleurs 1957). We use a position angle for the bar of  $120^\circ$ .

It is not clear, at this point, how great an influence the bar exerts over the dynamics of the surrounding gas and stars. In many barred galaxies, the bars sweep up gas and drive it towards the center (Kenney 1996; Ho, et al. 1996; Sakamoto et al. 1999). In our own Galaxy, the kinematics of gas in the inner regions is strongly influenced by the putative bar (Weiner & Sellwood 1999). While there is evidence for non-axisymmetric flows in the vicinity of the bar (Dottori, et al. 1996; Odewahn 1996), indicating that the bar may be dynamically important, the HI maps of Kim et al. show that the LMC bar does not dominate the central dynamics. From this we conclude that the mass of the bar cannot exceed the disk mass in the central regions, which leads us to a bound on the bar mass. Now,  $\sim 25\%$  of the disk mass lies within one scale length, while most of the bar lies in this same central region. We thus arrive at the following restriction:  $M_b < 25\%M_d$  to avoid bar domination. This agrees nicely with the estimates of Sahu (1994b), who suggested a bar to disk mass ratio in the range 15-20% based on luminosity considerations.

### 3.3. LMC Velocity Distribution and Vertical Scale Height

Now we turn to the velocity distribution of the model stars. Perhaps the best determination of the inner velocity curve of the LMC is in the work of Kim et al. (1998). When supplemented by outer rotation curves derived from carbon stars (Kunkel et al. 1997) and clusters and planetary nebulae (PNe) (Schommer, et al. 1992) the basic outline is clear: the circular velocity rises rapidly in the first two kpc and then levels off and is flat at about 70 km/s out to at least 8 kpc. There are indications of a possible dip at 3 kpc though this may not be significant. For our models we approximate the rotation curve by solid body rotation out to a radius  $r_{solid} = 2$  kpc, followed by flat rotation at  $v_c = 70$  km/s.

These studies help to define the bulk motions of gas and stars in the LMC. However, as Gould (1995) has shown, velocity dispersions (and the implied scale heights) are crucial in determining the optical depth and rate of microlensing. So let us consider measurements of the velocity dispersion of LMC populations. Prevot, Rousseau & Martin (1989) studied late-type supergiants and HII regions, concluding that the internal velocity dispersion of this population is approximately 6 km/s. This is quite close to that of the HI gas, 5.4 km/s (Hughes et al. 1991) which is hardly surprising as these tracers all belong to a very young population. A somewhat older population is probably illustrated by the disk-like ( $\sigma_v \sim 10$  km/s) CH stars found by Cowley & Hartwick (1991) which seem to correspond to ‘‘CH-like’’ stars found in the Galactic disk (Yamashita 1975). Cowley & Hartwick also found, however, a population with a considerably higher velocity dispersion (20-25 km/s), that presumably corresponds to an even older population. Meatheringham et al. (1988), in a study of planetary nebulae (PNe), found that the intermediate population of stars represented by the PNe are rotating as fast and in the same disk as the gas, but with a velocity dispersion of 19.1 km/s. Bessel et al. (1986) observed old (age  $\sim 10^{10}$  yrs) long period variables (OLPV’s), which are thought to trace the oldest stellar populations, and obtained a mean line-of-sight velocity dispersion of about 30 km/s. Hughes et al. (1991) also observed OLPV’s and obtained similar results ( $\sigma \sim 30$  km/s). We note here, for future reference, that a spheroidal distribution would require velocity dispersions of  $\sigma \approx v_c/\sqrt{2} \approx 50$  km/s. Since the observed dispersions of the OLPV’s fall far short

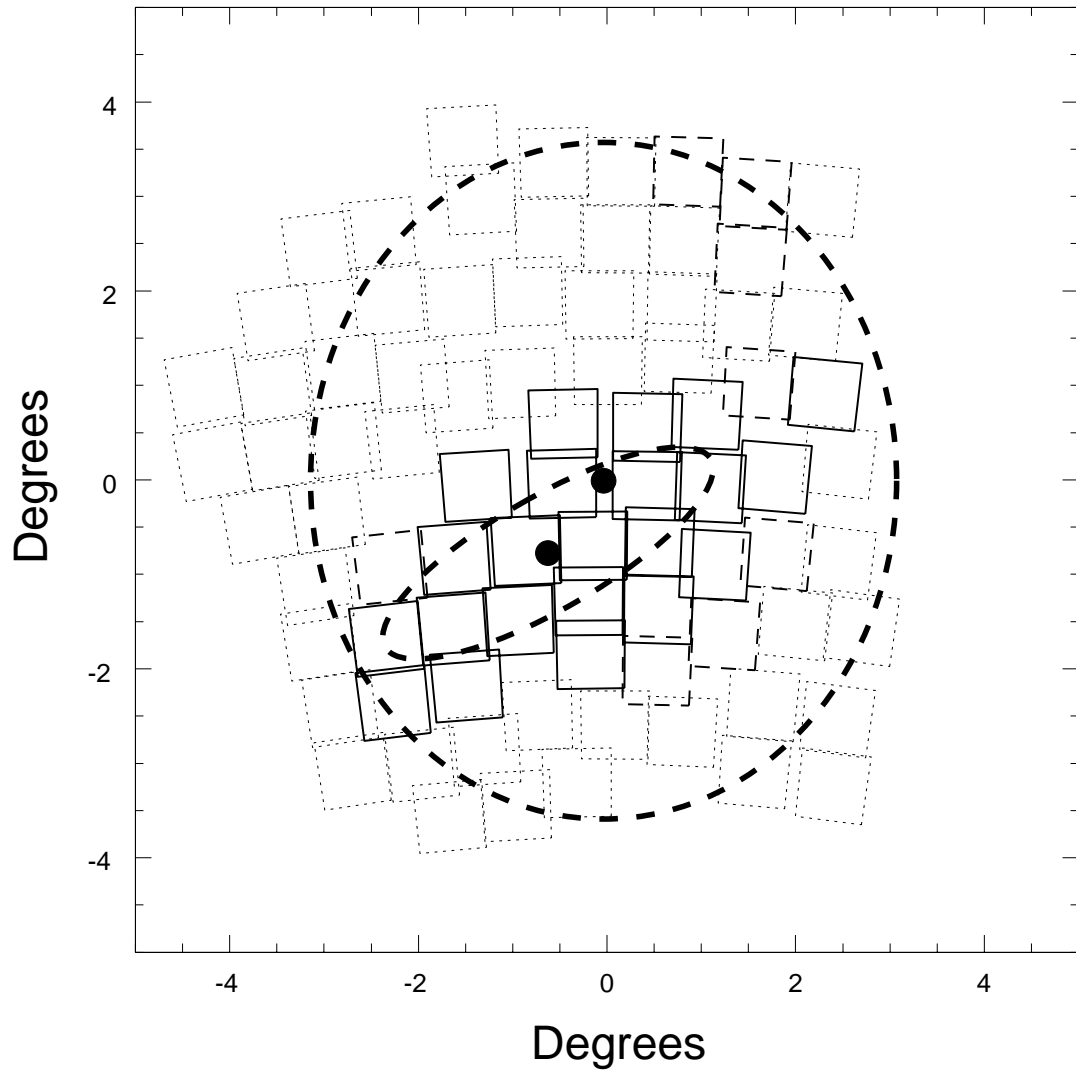


Fig. 1.— MACHO fields. The solid outline squares depict the 22 MACHO fields reported in Alcock et al. (1997a). The dashed squares are the 8 additional fields MACHO will report in their year 5 paper, and the dotted squares are the other 52 fields that they monitor. The thick dashed ellipses show the position and orientation of our model disk and bar. They are plotted at two scale lengths.

Population	Study	Velocity Dispersion	Age
supergiants	Prevot, Rousseau & Martin (1989)	6	young
HII	“	6	young
HI	Hughes et al. (1991)	5.4	young
VRC	Zaritsky & Lin (1997)	18.4	young?
PNe	Meatheringham et al. (1988)	19.1	intermediate
OLPV	Hughes et al. (1991)	33	old
ILPV	“	25	intermediate
YLPV	“	12-15	young
OLPV	Bessel et al. (1986)	30	old
metalpoor giants	Olszewski et al. (1993)	23-29	old
metalrich giants	“	16.0	intermediate?
new clusters	Schommer et al. (1992)	20	intermediate
old clusters	“	30	old
carbon stars	Kunkel et al. (1997)	15	young
CH stars (disk)	Cowley & Hartwick (1991)	10	yng/intermed?
CH stars (halo)	“	20-25	old

Table 1: Observed velocity dispersions for various populations.

of this, we see that even this oldest population derives much of its support from rotation, and therefore exhibits “disk-like” kinematics.

The general trend among the many kinematic studies of the LMC seems to be clear: tracers have velocity dispersions ranging from  $\sim 5$  km/s for very young ages to  $\sim 30$  km/s for the most ancient populations. *All* LMC populations studied to date have disk-like kinematics regardless of age (Olszewski et al. 1996). Table 1 lists some of the more recent kinematic studies of the LMC by population type, velocity dispersion and probable age.

From the velocity dispersions, let us now turn to the vertical scale heights. Bessel et al. (1986) estimated the vertical scale height of the oldest population to be roughly 0.3 kpc, while Hughes et al. (1991) estimated the scale height to be  $\lesssim 0.8$  kpc. They emphasized that this was the oldest population, accounting for at most 2% of the mass of the LMC. The majority of the LMC disk, they contend, should possess a more compact vertical distribution and smaller vertical velocity dispersions. This is supported by RR Lyrae and cluster studies which suggest that the ancient extended populations make up considerably less than 10% of the LMC stars (Olszewski et al. 1996; Kinman et al. 1991). We thus allow our scale height (which should characterize the bulk of the LMC population) to range up to 0.5 kpc and adopt velocity dispersions in a corresponding range of 10-30 km/s. In theory these parameters should be tied together

by the vertical Jeans equation (however see Weinberg 1999). In practice, our knowledge of the total mass and mass distribution of the LMC is poor enough that we simply note that the opposite extremes of these ranges (i.e. 10 km/s with 0.5 kpc and 30 km/s with  $< 0.2$  kpc) are likely inconsistent.

### 3.4. LMC Halos: Light and Dark

The above distributions describe the known stellar populations. We again reiterate that the non-detection of any stellar halo population ( $\sigma_v \sim 50$  km/s) places severe constraints upon the existence of such a stellar halo. The above noted RR Lyrae and cluster studies, along with the OLPV observations limit the stellar halo to perhaps 5% of the mass of the LMC (Hughes et al. 1991; Olszewski 1993; Olszewski et al. 1996; Kinman et al. 1991).

This, however, places no limits upon the existence of a dark halo, to which we now turn. Obviously, even less is known about the LMC dark matter than its luminous populations. As Kim et al. (1998) discuss, the observed LMC rotation curve is inconsistent with the distribution of known populations, given the assumption of a *constant* mass to light ratio. Schommer et al. (1992) obtain similar results. Although the variation in the mass to light ratio required to explain the rotation curve with luminous matter alone is less than a factor of two, we can take these results as *prima facie* evidence for dark matter within the LMC.

This should not be too surprising, since studies of the velocity curves of similar dwarf galaxies show that they are dominated by dark matter (see e.g. Carignan & Purton 1998). Models without dark halo also exist that can explain the rotation curves (D. Alves 1999, private communication), but these will not be discussed here. There are numerous models that have been used to describe dark matter in galaxies. Most common, and perhaps easiest, is the simple spherical pseudo-isothermal distribution,

$$\rho_h = \rho_0 \left[ 1 + \frac{r^2}{a_h^2} \right]^{-1}$$

with core radius  $a_h$  and central density  $\rho_0$ . In the limit  $a_h \rightarrow 0$ , this distribution gives an isothermal Maxwellian velocity profile (Binney & Tremaine 1987). For the LMC, however, core radii smaller than  $a_h \sim 1$  kpc lead to problems matching the rotation curve. Although not self-consistent, for simplicity we use  $a_h > 1$  kpc and a uniform Maxwellian velocity distribution. We take the fraction of this halo in MA-CHOs to be  $f_M$ .

Since the LMC is embedded in the (dominating) gravitational potential of our Galaxy, we expect the LMC to have a tidal radius, beyond which objects are not stably bound to the LMC (Binney & Tremaine 1987). This places a limit on the size of the LMC halo. Although the density should smoothly decline to zero near the tidal radius, for simplicity we instead implement a truncation radius,  $r_t$ , beyond which the LMC halo density abruptly vanishes. Using star counts from the 2MASS survey, Weinberg (1998) has estimated  $r_t \approx 11$  kpc. This is the value we adopt.

### 3.5. LMC Mass

The question of the LMC mass is an unsettled one. A few of the more recent mass estimations are shown in Table 2. Estimates range from only a few  $\times 10^9 M_\odot$  to  $\sim 2 \cdot 10^{10} M_\odot$ . Close inspection, however, reveals a few regularities. The highest estimates are based of the spheroidal estimator of Bahcall & Tremaine (1981), which assumes both velocity isotropy and a spherical mass distribution. Since both of these conditions are likely to be violated, the spheroidal estimators should be taken as upper limits. A similar argument can be made for the point mass estimation of Kunkel et al. (1997). With these caveats in mind the data seem consistent with a disk of perhaps  $3 \cdot 10^9 M_\odot$  and a halo whose mass within 8 kpc is

roughly  $6 \cdot 10^9 M_\odot$ . While the extremely high quality HI data of Kim et al. (1998) would appear to rule out a disk mass much in excess to this, the halo component is much more uncertain. We thus take  $M_{disk} + M_{bar} \leq 5.0 \cdot 10^9 M_\odot$  and allow the total LMC halo mass within 8 kpc to range up to  $1.5 \cdot 10^{10} M_\odot$ . In figure 2 we show the rotation curves associated with several choices of component masses. While our preferred parameters fit the observed velocity profile quite nicely, the upper ends of our allowed ranges are clearly starting to run afoul of the observations.

This covers all of the populations we consider for LMC self lensing. The various parameters and their preferred values are listed in Table 3. However, since observations are subject to change, it is worthwhile to consider not only the currently preferred description of the LMC, but a wide class of models and parameters, so that future observations easily translate into microlensing predictions. We have therefore also indicated the acceptable range of each model parameter in Table 3. Of course, models that simultaneously take extreme values of all the parameters may not be realistic. While this range *spans* the set of acceptable models, not all models in this range are acceptable.

## 4. Calculations

Using the models specified in the previous section, the microlensing event rate, optical depth, and timescale distribution can be calculated. The microlensing rate is the number of events per year per star. To obtain the total number of events expected for an experiment one would multiply the rate by the observational exposure, which is defined as the num-

Parameter	Preferred Value	Allowed Range
inclination	30°	20 – 45°
$R_d$	1.8°	1.8°
$z_d$	0.3 kpc	0.1-0.5 kpc
$v_c$	70 km/s	60-80 km/s
$L$	50 kpc	45-55 kpc
$\sigma_v$	20 km/s	10-30 km/s
$a_h$	2 kpc	1-5 kpc
$M_{d+b}(8\text{kpc})$	$3 \cdot 10^9 M_\odot$	$< 5 \cdot 10^9 M_\odot$
$M_{dark}(8\text{kpc})$	$6 \cdot 10^9 M_\odot$	$< 1.5 \cdot 10^{10} M_\odot$
$M_{bar}/M_{d+b}$	0.15	0.05-0.25
$M_{stellar\ halo}$	$0 \cdot 10^8 M_\odot$	$0 - 5.0 \cdot 10^8 M_\odot$

Table 3: Model parameters.  $M_{d+b} = M_{disk} + M_{bar}$ . All masses are for LMC distances of 50 kpc

Study	Mass Estimate	Radius	Component	
Hughes et al. (1991)	$6.0 \cdot 10^9 M_\odot$	4.5 kpc	Total	Spheroidal estimator
Kim et al. (1998)	$2.5 \cdot 10^9 M_\odot$		Disk	Rotation curve fit
“	$3.4 \cdot 10^9 M_\odot$	8 kpc	Halo	
Schommer et al. (1992)	$\sim 2.0 \cdot 10^{10} M_\odot$	5 kpc	Total	Spheroidal estimator
“	$1.0 \cdot 10^{10} M_\odot$	8 kpc	Total	Rotation estimate
Meatheringham et al. (1988)	$3.2 \cdot 10^9 M_\odot$		Disk	Rotation maximum fit
“	$6.0 \cdot 10^9 M_\odot$	5 kpc	Total	
Kunkel et al. (1997)	$6.2 \cdot 10^9 M_\odot$	5 kpc	Total	Point mass estimation
“	$< 1.0 \cdot 10^{10} M_\odot$		Total	

Table 2: Estimates of the LMC mass. Note that some entries refer to specific components, such as the disk or halo, while other entries correspond to the LMC as a whole.

ber of monitored stars times length of time they were monitored. The optical depth is the probability that a given source star is lensed with magnification greater than 1.34.

The optical depth along a given line of sight is given by

$$\tau = \frac{1}{N_s} \int_0^\infty dL n_s(L) \int_0^L dl \pi R_E^2(L, l) n_l(l)$$

where  $n_s$  is the number density of sources,  $n_l$  is the number density of lenses,  $R_E$  is the Einstein radius defined above,  $L = D_{OS}$  is the distance to the source, and  $N_s = \int n_s dL$  is the total number of sources along the line of sight. Writing  $\rho(\vec{x}) = \langle m \rangle n_l(\vec{x})$  and inserting the expression for the Einstein radius  $R_E$  gives

$$\tau = \frac{4\pi G}{c^2 N_s} \int_0^\infty dL n_s(L) \int_0^L dl \frac{l(L-l)}{L} \rho_l(l).$$

Before proceeding further, we discuss the source distribution in more detail. In the simplest approach the source density would be set to the mass density (disk+bar) we have already discussed. This ignores two important issues. First, the LMC is seen almost face-on, and hence the thin dust and gas disk obscures the far half of the stars. This preferentially removes source stars with the highest optical depth, lowering the observed optical depth. Modeling the extinction as a zero thickness plane of 0.4 V-magnitudes (Oestricher & Schmidt-Kaler 1996), a rough approximation shows that the effect should reduce the optical depth by about 15% for disk-disk self lensing. In the following we ignore this effect, simply noting that our quoted results are over-estimates. The second issue concerns the differing populations of the disk and bar. These different populations (due to the varying ages

and star formation history) yield different source to mass ratios. Unfortunately, with the present knowledge of the bar and disk luminosity functions and relative metallicities etc. a precise calculation is impossible. We therefore assume a uniform mass to source ratio.

We have found it convenient to calculate the optical depth, event rate, and duration distribution using a Monte Carlo method. One advantage of the Monte Carlo technique is that it easily allows consideration of arbitrary spatial distributions of lenses and sources. Another important advantage of the Monte Carlo method is the ease with which we were able to average over the experimental fields as discussed in the following section. In addition, the separate integrals for the optical depth, rate, and event timescales can all be evaluated simultaneously, in one fell swoop.

#### 4.1. MACHO Fields

For self lensing models the optical depth varies rapidly with position in the LMC. Thus a single number, “the optical depth to the LMC” is only useful if the precise location of the observed sources is specified. In order to make the comparison to the observed optical depth we have chosen to average our results over the MACHO collaboration fields (Alcock, et al. 1997a). Ideally we should fold in the experimental efficiency and relative source numbers in each field as observed. Since these numbers are unavailable, however, we have weighted each field by the *model* number of stars. We show in Figure 1 the fields over which the optical depth is averaged. The solid outlines depict the 22 fields covering about 10 square degrees used in the MACHO year 2 analysis (Alcock, et al. 1997a). Note that the year 2 fields are concentrated along the



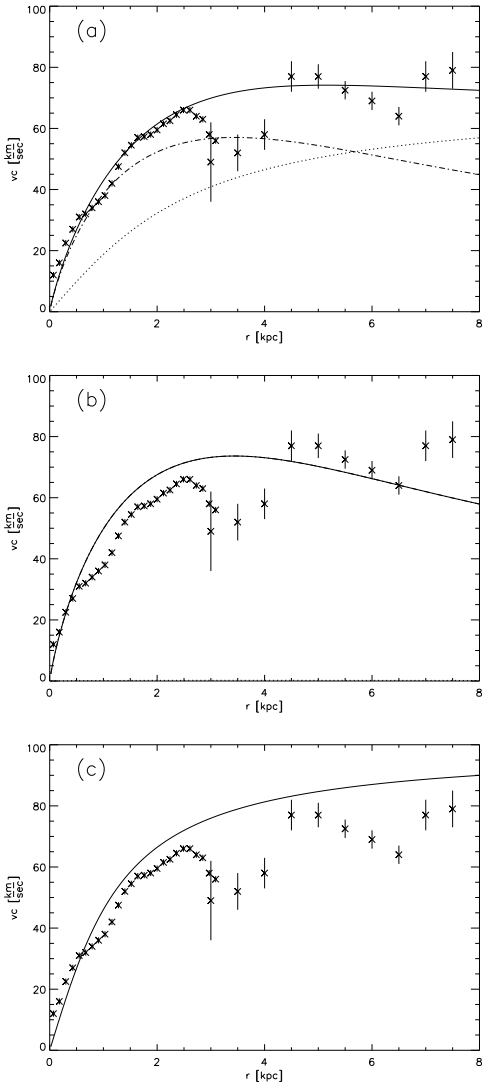


Fig. 2.— Model rotation curves. The plotted points with error bars are from Kim et al. (1998) and Kunkel et al. (1997). Panel (a) shows the predicted rotation curve for our preferred model, with  $M_{disk} = 3 \cdot 10^9 M_{\odot}$  (entirely in the double exponential disk),  $M_{dark}(8 \text{ kpc}) = 6 \cdot 10^9 M_{\odot}$  and  $a_h = 2.0 \text{ kpc}$ . The dash-dot line shows the disk contribution, and the dotted line shows the halo contribution. Panel (b) shows the predicted rotation curve for the maximal disk we allow,  $M_{disk} = 5 \cdot 10^9 M_{\odot}$ . Note that it already significantly overshoots the observed velocities. Any additional dark component exacerbates the problem. Panel (c) shows the curve for the maximum dark halo mass,  $M_{dark}(8 \text{ kpc}) = 1.5 \cdot 10^{10} M_{\odot}$  and  $a_h = 1 \text{ kpc}$ . Clearly, masses in excess of this can safely be ruled out.

regions of highest numbers of source stars. The dotted outlines describe the roughly 40 square degrees (82 fields) that are being monitored by the MACHO collaboration.<sup>1</sup> These cover most of the LMC disk out to a radius of 3.5 degrees from the center (about 2 disk scale lengths). Later we will discuss possible observational consequences of the increased coverage. Also of interest are the 30 fields that will be presented in the MACHO collaboration 5 year analysis (Vandehi 1998). We note that the EROS II collaboration is similarly observing most of the LMC disk, while the OGLE II collaboration monitors 4.2 square degrees (Udalski, *et al.* 1997).

#### 4.2. Mass function

Although the optical depth is independent of the mass function, the event rate and the timescale distribution do depend upon the lens masses. We therefore must consider an appropriate mass function for the lensing population. As we expect the rate to be dominated by low mass stars, we choose to employ the MF derived by Gould, Bahcall & Flynn (1997), which they based upon counts of M dwarfs in the MW disk. Gould et al. found that

$$\frac{dN}{dm} \propto \left( \frac{M}{0.59 M_{\odot}} \right)^{\alpha},$$

with  $\alpha \approx -0.56$  for  $m < 0.59 M_{\odot}$  and  $\alpha \approx -2.21$  for  $m > 0.59 M_{\odot}$ . Since the timescales and rate are dependent only on the square root of the masses the precise details of the LMC mass function are not important unless it is radically different from that of the MW.

### 5. Results

The measured total optical depth towards the LMC from the 2-year MACHO collaboration analysis is  $2.9_{-0.9}^{+1.4} \cdot 10^{-7}$  (Alcock, et al. 1997a). How does this compare with the predicted range of optical depths of the above models?

#### 5.1. Disk/Bar Optical Depth and Scalings

Let us first consider disk-disk lensing. Evaluating the integral, and plugging in the preferred disk parameters listed in Table 3, we obtain a (22) field averaged optical depth of  $\tau = 1.46 \cdot 10^{-8}$  for disk-disk lensing.

<sup>1</sup>The centers of all 82 fields can be accessed from the MACHO collaboration web site, at <http://wwwmcho.mcmaster.ca/>

This is the best value for the disk-disk optical depth, given the current status of observations. As noted, however, we should explore the dependence of  $\tau$  upon the model parameters. We can obtain a reasonable scaling using a simple-minded argument. Let's first consider the optical depth for a single source star at the LMC center. This integral is easy to do exactly, but for our purposes we are interested in its asymptotic behavior. Writing the integral in dimensionless form, we see it is approximately  $\propto \rho_0 \int e^{-Ax} x dx \propto \rho_0 A^{-2}$ , where  $\rho_0 = M_{disk}/(4\pi R_d^2 z_d)$  is the central density and

$$A = L \left( \frac{\cos i}{z_d} + \frac{\sin i}{R_d} \right)$$

is the only other form in which these parameters enter the integral. The extended source distribution will modify this scaling, but for disk-disk lensing, the source distribution enters the line-of-sight integral again in the form of  $A$ . Thus,  $\tau \sim \rho_0 L^2 F(A)$  should capture the essential behavior of the 3-d averaged optical depth, with asymptotic leading behavior  $\tau \propto \rho_0 A^{-2}$ . For the LMC,  $A \approx 160$ , so we expect the expansion

$$\tau \propto \frac{M_{disk} L^2}{R_d^2 z_d A^2} (1 + a_1 A^{-1} + a_2 A^{-2} + \dots)$$

to describe accurately the scaling of the optical depth with the parameters over the range of interest, even if we keep only the first one or two terms. However, for estimation purposes, the leading behavior will be good enough.

We arrive at an interesting relation if we further approximate this already zeroth-order treatment. For a nearly face-on, thin disk,  $A \approx L \cos(i)/z_d$ . Then  $\tau \propto M z_d / (R_d^2 \cos^2 i)$ . Note that a similar result was derived by Sahu & Sahu (1998). Now, quantities such as  $M, R_d$ , etc. are derived, not measured directly. They are inferred from measured parameters such as the apparent axis ratio  $k = \cos i$ , the rotation curve (which itself is derived from radial velocity measurements), the distance  $L$ , and the vertical velocity dispersion  $\sigma_z$ . For example, the vertical scale height  $z_d$  is typically computed using the Jeans equations, which for a self-gravitating thin disk in equilibrium demand that  $z_d \sim \sigma_z^2 / \Sigma$ , where  $\Sigma$  is the local surface density. Inserting this into our scaling for  $\tau$  gives

$$\tau \propto \frac{\sigma_z^2}{\cos^2 i}.$$

This, of course, is Gould's (1995) analytic result. Gould's point is that for disk-disk lensing, to lowest order, the distance of the LMC and the total mass (rotation curve) are irrelevant; that is, the only directly observed quantities that seem to matter are the velocity dispersion and axis ratio. It is important to keep in mind that this conclusion is predicated upon the validity of the self-gravitating, thin-disk, steady-state solutions to the Jeans equations, which Weinberg (1999) has argued may not be applicable to the LMC. We feel that it is better to base microlensing estimates upon parameters like the scale height, that are directly tied to the spatial density distribution, rather than quantities like the velocity dispersion, which require questionable assumptions.

The optical depths and expected scalings for the other three cases – bar-disk, bar-bar, disk-bar – can be computed with similar ease. For our preferred set of parameters, we find  $\tau_{bd} = 1.25 \cdot 10^{-8}$ ,  $\tau_{bb} = 1.37 \cdot 10^{-8}$ ,  $\tau_{db} = 8.7 \cdot 10^{-9}$  (22 fields). Again, we may also be interested in these optical depths for different parameter values, so let's consider the scaling behavior of these integrals. Now, we previously derived an approximate form by considering the limit of a compact source distribution and diffuse lens distribution. What if we reverse the situation, and instead imagine a compact lens distribution and extended source distribution? For definiteness, consider a single lens at the LMC center, lensing background stars with density profile  $\rho_s$ . In addition, let  $\rho_s$  be strongly peaked about the LMC center. Then the optical depth takes the approximate form  $\tau \propto \int dl \rho_s(l) L l / (L + l) \sim L^2 \int \rho_s x dx$ , the exact same form we derived earlier, but with  $\rho_s$  replacing  $\rho_l$ . This should not be surprising, since in the limit  $D_{OS} \approx D_{OL}$ , the Einstein radius becomes a function only of  $D_{LS}$ . Since only the relative distance from source to lens matters,  $\tau$  becomes (in some sense) symmetric in  $\rho_s$  and  $\rho_l$ . To sum up, when both the source and lens distributions are compact, but the source distribution is more compact, we expect  $\tau \propto L^2 \int \rho_l x dx$ , and when the lens distribution is more compact then  $\tau \propto L^2 \int \rho_s x dx$ . For true self-lensing (disk-disk or bar-bar) these expressions are identical.

With these ideas in mind, we can now work out the approximate scalings. Let's first consider bar-bar lensing. The dimensionless integral in this case behaves, to leading order, like  $\int e^{-Bx^2/2} x dx \sim B^{-1}$ ,

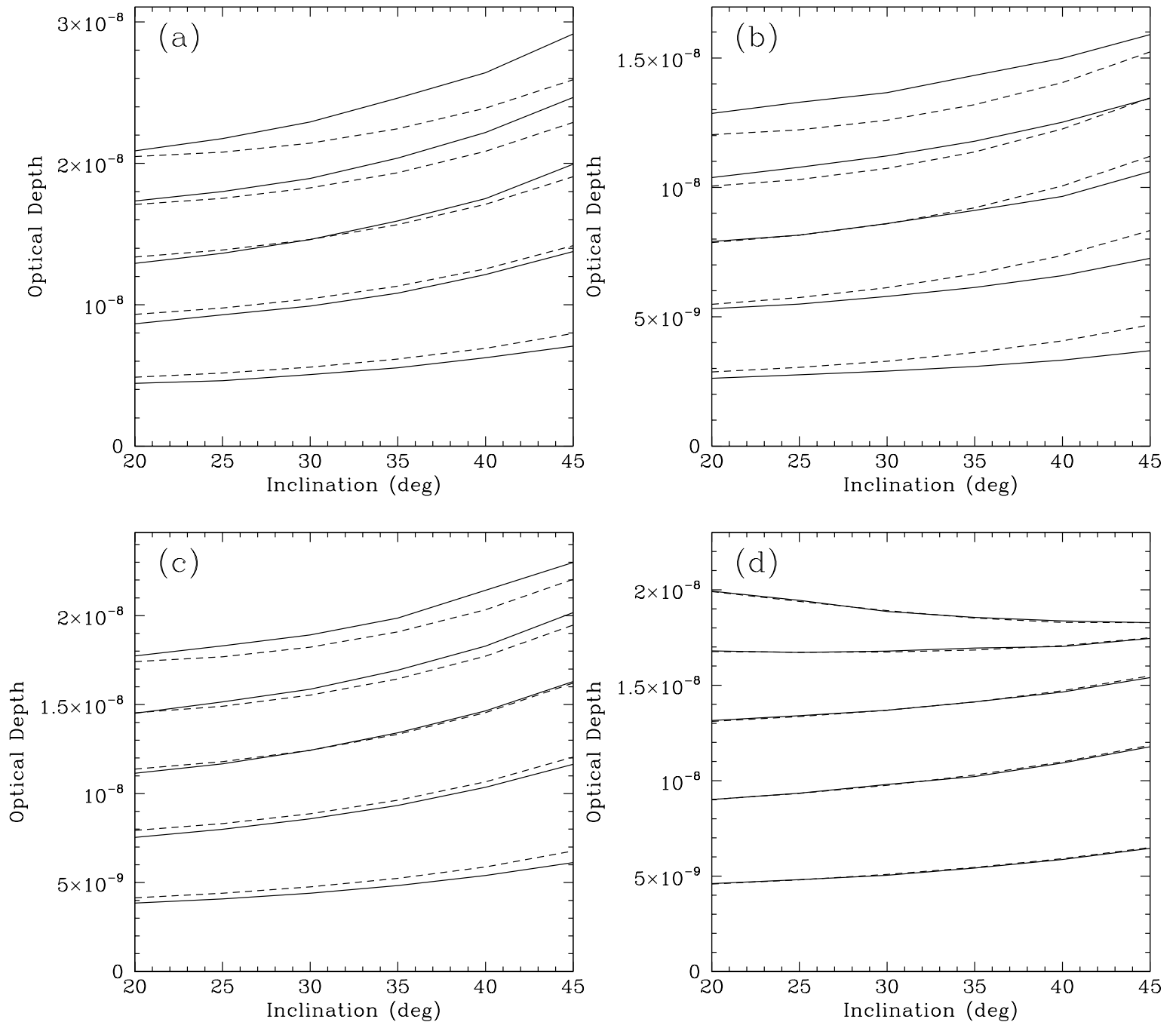


Fig. 3.— Variation of optical depth with model parameters. Panel (a) is for disk-disk, (b) is disk-bar, (c) bar-disk, and (d) bar-bar. The solid lines are the results of our numerical calculation of  $\tau$ , for vertical scale height  $z = 0.1, 0.2, 0.3, 0.4, 0.5$  from bottom to top. All other parameters were set to their preferred values. The dashed lines are the predicted values using the scalings described in the text, for the same parameters. As expected, the scaling is most accurate for bar-bar, where both the source and lens distributions are compact.

where

$$B = L^2 \left[ \frac{\cos^2 i}{z_b^2} + \sin^2 i \left( \frac{\sin^2 \psi}{x_b^2} + \frac{\cos^2 \psi}{y_b^2} \right) \right],$$

and  $\psi$  is related to the bar's position angle on the sky by  $\tan(\text{PA}_{\text{bar}} - \text{PA}_{\text{disk}}) = \tan(\psi) \cos(i)$ . Thus,  $\tau$  scales roughly like

$$\tau \propto \frac{M_{\text{bar}} L^2}{x_b y_b z_b B}.$$

Now we turn to the cross terms (disk-bar and bar-disk). Clearly, the bar Gaussian distribution is more compact than the disk double exponential distribution, so we expect both of these terms to have the disk scaling.

Figure 3 shows the calculated optical depths averaged over 22 fields, as a function of various parameters, as well as the predictions from the scaling laws (normalized to match at the preferred parameters). In general the scalings are reasonably accurate. The scalings work about as well for the 30 field set and the 82 field set. For an order of magnitude estimate, one can use pure disk-disk with the sub-zeroth order scaling given above, namely

$$\tau \approx 1.7 \cdot 10^{-8} \left[ \frac{z_d}{0.3 \text{ kpc}} \right] \left[ \frac{M}{3 \cdot 10^9 M_\odot} \right] \times \left[ \frac{R_d}{1.6 \text{ kpc}} \right]^{-2} \left[ \frac{\cos(i)}{\cos(30^\circ)} \right]^{-2}.$$

For the 82 field sample the scaling is the same but the prefactor is 1.05, while for the 30 field sample it is 1.33. A complete average over the LMC disk out to very large radii would give a prefactor of 0.72.

The total optical depth for a particular set of model parameters is somewhat involved to calculate. Since the spatial distribution of the various source populations is different one cannot simply add together the mass weighted average optical depths. Instead, one needs to add the optical depths weighted at the field level and then calculate the total optical depth from the field values. No combination of parameters within our ranges allows an optical depth greater than  $8.0 \cdot 10^{-8}$ . For the preferred values the optical depth is  $2.4 \cdot 10^{-8}$ . Note that this value is *ten times* smaller than the observed optical depth.

## 5.2. Timescales

Figure 4 shows the timescale distribution for our preferred disk/bar model, not including any LMC

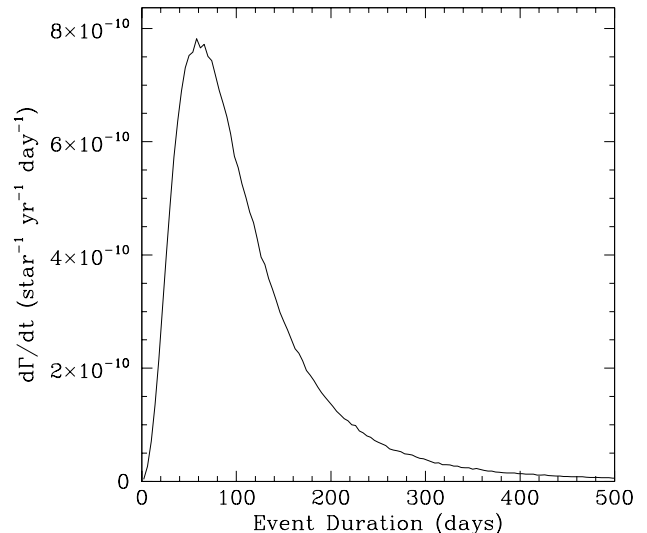


Fig. 4.— Timescale distribution averaged over 22 fields for our preferred model. See text for more details.

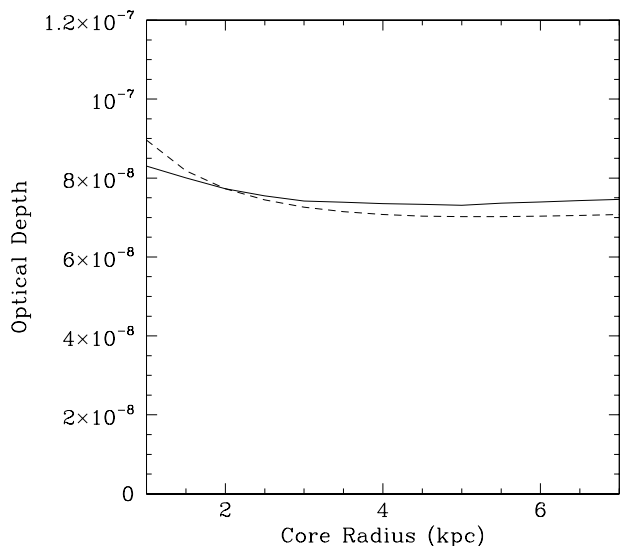


Fig. 5.— Optical depth as a function of halo core radius. The halo is taken to be 100% MACHOs with a mass of  $6.0 \cdot 10^9 M_\odot$  within 8 kpc. The source distribution is our preferred disk/bar model. Note how insensitive the optical depth is to the core radius. The dashed line shows the scaling described in the text.

halo contribution, using the mass function from Gould et al. (1997). The efficiency weighted average event duration  $\langle \hat{t} \rangle = 101$  days. This is consistent with the observed  $\langle \hat{t} \rangle$  of 84 days (Alcock, et al. 1997a), given the observational uncertainties and our lack of knowledge of the precise details of the mass function and velocity distribution. This profile is fairly uniform over the face of the LMC.

### 5.3. LMC Halo optical depth

We have also calculated the optical depth due to a possible LMC MACHO halo. The optical depth is shown in Figure 5 as a function of the halo core,  $a_h$ . If the mass of the halo is varied the optical depth scales linearly. The values shown are for a  $6 \cdot 10^9 M_\odot$  LMC halo 100% composed of MACHOs. We find values of the optical depth between  $\sim 7.5 \cdot 10^{-8}$  and  $\sim 8.5 \cdot 10^{-8}$  depending on parameters. It is clear that a halo type configuration is much more effective at producing optical depth than the disk/bar. Now, there are at least two possible types of LMC halos, both of which could, conceivably, be present simultaneously. First, a dark matter halo, common in dwarf galaxies, is possible. The composition of such a halo should be similar to the composition of the Milky Way halo (i.e. unknown!). If the MW halo has a fraction  $f_M$  of MACHOs (the remainder presumably consisting of some exotic non-baryonic material), then the LMC halo might have a similar fraction. If so, then microlensing of the LMC halo lenses would constitute discovery of dark matter, but the implied halo fraction would depend upon the mass of LMC halo (Weinberg 1998; Kerins & Evans 1999). That is, the predicted optical depth of the MW halo plus LMC halo would be roughly  $\tau \simeq f_M(4.7 \cdot 10^{-7} + [0 - 2.3] \cdot 10^{-7})$ , and so the effect of including a dark LMC halo would be to reduce the derived MACHO halo fraction by  $\Delta f_M / f_M = -[0 - 2.3] / (4.7 + [0 - 2.3]) = -[0\% - 33\%]$ . Using the current estimate  $f_M$  of 50% (Alcock, et al. 1997a), inclusion of an LMC halo lowers  $f_M$  to somewhere in the range [33% - 50%].

The other type of possible LMC halo is a stellar halo with a luminosity function similar to that in the disk. This could consist of stars stripped from the disk (Zaritsky & Lin 1997; Weinberg 1999) or something corresponding to the spheroid of the Milky Way. This is the halo of interest in creating a non-dark matter explanation for LMC microlensing. As discussed above, the mass of such a halo is tightly constrained by numerous observations.

As before, we can work out an approximate scaling for the optical depth of LMC halo lensing. The halo distribution is definitely less compact than the source distribution, so  $\tau \propto L^2 \int \rho_l x dx$ . Let  $a_h$  be the halo core radius,  $r_t$  the tidal radius (actually truncation radius),  $\rho_0$  the halo central density, and  $L$  the distance to the LMC. Then the optical depth should scale like

$$\tau_h \propto \rho_0 a_h^2 \left[ \frac{1}{2} \log \left( 1 + \frac{r_t^2}{a_h^2} \right) + \frac{\tan^{-1}(r_t/a_h)}{L/a_h} - \frac{r_t}{L} \right].$$

### 5.4. Total Optical Depth

All of the above components combine to give the total predicted optical depth for LMC/LMC self lensing. This averaging is not completely trivial since the density of source stars is different in each population. To find an average optical depth for a set of model parameters and a set of observed fields, the optical depths for each population should be multiplied by the source density at each field location and then averaged with this weighting. Even more realistically, observational effects such as stellar crowding and observation strategy will cause the monitored source objects to differ from the underlying stellar sources, and the detection efficiency of each field to vary, so additional corrections for each field should also be made. We blissfully ignore all such observational effects, and assume that our model source distribution approximates the true observed source distribution with uniform source exposure and detection efficiency. Table 4 shows a summary of the optical depths for the various populations discussed above and also the averaged totals. The ranges of parameters shown in Table 3 were used. We see that for our preferred parameters a total optical depth due to known LMC stellar populations of  $2.44 \cdot 10^{-8}$  is found, with values between  $0.47$  and  $7.84 \cdot 10^{-8}$  lying in our acceptable range.

### 5.5. Variation of Optical Depth across the face of the LMC

One potentially powerful way of distinguishing Milky Way (MW) halo microlensing from LMC self-lensing is to compare the spatial distribution of the observed microlensing events with the predictions of LMC and halo models (Alcock, et al. 1997a). For microlensing events due to a MW halo population of lenses, the lens population is uniform across the source distribution, so one expects the events to be distributed in proportion to the LMC source density times the experimental efficiency. For LMC/LMC self

Source/Lens geometry	Relative Weight			Preferred Values			Allowed Range (22 fields)
	22	30	82	22	30	82	
disk/disk	0.61	0.67	0.79	1.46	1.34	1.04	0.23-5.81
disk/bar	0.61	0.67	0.79	0.87	0.72	0.39	0.11-4.07
bar/disk	0.39	0.33	0.21	1.25	1.24	1.23	0.40-4.13
bar/bar	0.39	0.33	0.21	1.37	1.36	1.33	0.32-4.00
total bar+disk	1	1	1	2.44	2.24	1.67	0.47-7.84
(disk+bar)/dark halo	$f_M$	$f_M$	$f_M$	7.75	7.73	7.18	0 - 22.6

Table 4: Optical depths for LMC self lensing in units of  $10^{-8}$ , averaged over the 22 fields of Alcock et al. (1997a). The dark halo result is for a MACHO fraction  $f_M = 1$ . Note that the relative weights apply only to the preferred set of parameters.

lensing, both the sources and lenses are distributed like the LMC stars, so there should be a more rapid drop off of measured optical depth at large distances from the LMC bar.

In Figure 6 we show the predicted distribution of disk/bar optical depth (times the source density in the model) as a function of RA and declination across the face of the LMC for our self-lensing model, employing the preferred parameters. It is clear that the optical depth drops off rapidly with radius. We note that even a few events in the regions far from the bar can rule out the LMC/LMC self lensing hypothesis, if the LMC lens population is accurately modeled as a disk/bar. Figure 7 shows the same for LMC halo lensing. Note that the halo optical depth is much less concentrated than the corresponding disk/bar result. Interestingly, there is a slight east-west asymmetry for LMC halo microlensing due to the inclination of the disk. Although such an asymmetry would be virtually impossible to detect experimentally, in principle it could be used to discriminate between LMC halo and MW halo microlensing.

Looking at Figures 6 and 7, we see that the disk/bar distribution is qualitatively distinct from the halo distribution. We can quantify this observation using a simple measure. We write  $\tilde{\theta} \equiv \langle \theta_{ij} \rangle$ , where  $\theta_{ij}$  is the angle on the sky between the location of events  $i$  and  $j$ , and the average is over all pairs.  $\tilde{\theta}$  is a statistic that measures the average separation of events, and therefore the extent of the spatial distribution of events. It is easy to compute the experimental value,  $\tilde{\theta}_{obs}$ , from the observed events. It is similarly easy to compute the values predicted by any given model. Since the main feature of the event distribution that should help rule out models is the central compactness, we expect that  $\tilde{\theta}$  should measure

whether a model can reproduce the observed event distribution, in the same sense that a KS test would. Unfortunately, the paucity of actual events may limit our ability to rule out models based upon the observed event distribution. In addition, to be useful the monitored sources must span a sufficiently wide area, since obviously we will be unable to discern any intrinsic central concentration if the data sample only a small swath of the sky.

We have computed  $\tilde{\theta}$  for our models using both the 22 field sample and the 82 field sample. In order to give an estimate of the allowed range of  $\tilde{\theta}$ , we have plotted it for numerous random parameter sets picked uniformly in parameter space. Figure 8 shows a scatterplot of  $\tau$  versus  $\tilde{\theta}$  for LMC disk, LMC halo, and MW halo models. For the 22 field sample depicted in panel (a) the LMC disk/bar (x's) and the LMC halo (circles) models are resolved in both  $\tilde{\theta}$  and  $\tau$ , though the experimental uncertainties on  $(\tilde{\theta}_{obs}, \tau_{obs})$  plotted for the MACHO LMC 2 year data set do not allow them to be distinguished. We see that the selection effect of small sky coverage, in conjunction with low-number statistics, does not yet allow a clear choice of model based upon the event distribution. On the other hand, the 82 field sample plotted in panel (b) demonstrates strong separation of the model classes in both  $\tilde{\theta}$  and  $\tau$ . The 30 fields result is quite similar to the 22 fields plot, with a maximum range in  $\tilde{\theta}$  of  $\lesssim 2^\circ$  for halo lensing. Clearly, future data with increased sky coverage and more events will be a strong discriminant between disk models and halo models. Note, however, that the plots also indicate that the LMC halo and MW halo models will probably remain degenerate.

We now turn to a discussion of other self-lensing models that have been proposed recently.

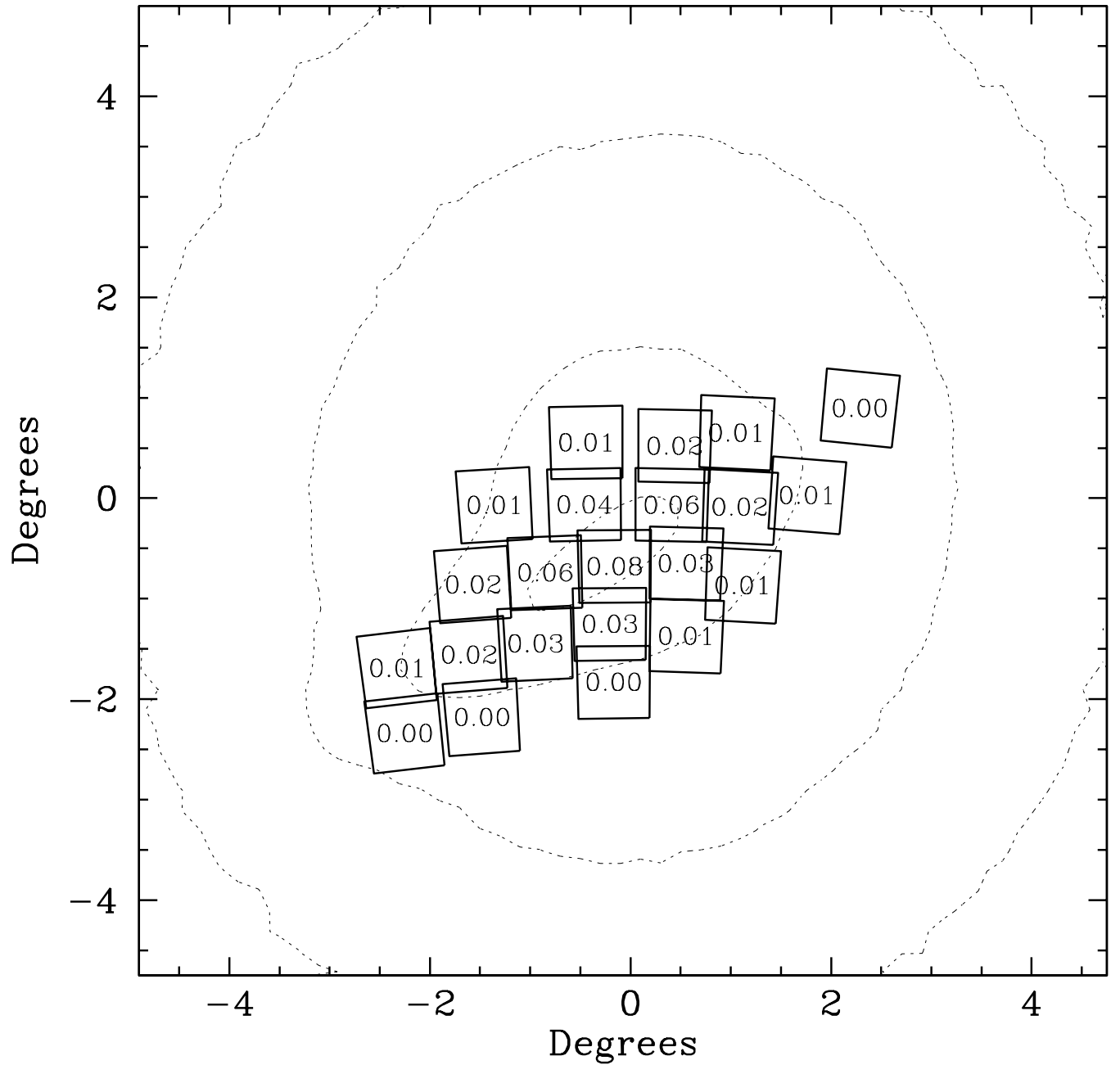


Fig. 6.— The dotted contours depict the optical depth times source number density as a function of position on the sky for LMC self-lensing, for our preferred model with both disk and bar. The contours are spaced by decades. The 22 fields are overlaid, along with the expected number of events using our preferred model, an exposure of  $1.82 \cdot 10^7$  star-years, and the detection efficiencies of Alcock et al. (1997a). We find a total of 0.44 expected events.

Paper	$M_{d+b}$	$M_{stellar\ halo}$	$z_d$	$\cos(i)$	$\tau_{paper}$	$\tau_{us}$
Sahu 1994	$2 \cdot 10^9 M_\odot$	0	$\sim 0.2\text{kpc}$	0	$5 \cdot 10^{-8}$	$5.3 \cdot 10^{-8}$
Gould 1995	$\sim 1.2 \cdot 10^9 M_\odot$	0	$\sim 0.2\text{kpc}$	$27^\circ$	$\lesssim 10^{-8}$	$\sim 7.6 \cdot 10^{-9}$
Alcock, <i>et al.</i> 1997a	$6.8 \cdot 10^9 M_\odot$	0	0.25 kpc	$30^\circ$	$3.2 \cdot 10^{-8}$	$3.2 \cdot 10^{-8}$
Aubourg 1999	insignificant	$\sim 1.4 \cdot 10^{10} M_\odot$	-	-	$1.3 \cdot 10^{-7}$	$1.2 \cdot 10^{-7}$
Weinberg 1999	$10^{10} M_\odot$	0	$\sim 0.4\text{kpc?}$	$45^\circ$	$1.4 \cdot 10^{-7}$	$1.4 \cdot 10^{-7}$
This work	$3 \cdot 10^9 M_\odot$	0	0.3 kpc	$30^\circ$	$2.44 \cdot 10^{-8}$	$2.44 \cdot 10^{-8}$

Table 5: Summary of LMC self lensing optical depths results for various groups. See text for more explanation. Gould’s, Aubourg’s & Weinberg’s results are all for a single line-of-sight, which overestimates the 22 field averaged optical depth by  $\sim 50\%$ . Sahu’s model was pure bar, with no disk. Gould’s optical depth was expressed in terms of the vertical velocity dispersion; we chose values of the disk mass and scale height which roughly give that dispersion. It is unclear what scale height corresponds to Weinberg’s calculation, but 0.4 kpc is a reasonable estimate.

## 5.6. Other Models

The models of Sahu (1994a,b), Gould (1995), Alcock, *et al.*(1997a), Aubourg, *et al.*(1999), are all contained within the framework we have explored. The main differences between the results of these different workers come from different choices of LMC model and LMC model parameter. In Table 5 we show a summary of the LMC self-lensing results of several previous workers along with the parameters they chose. We also show an approximation of their models within our framework. Note in every case, the predicted optical depth can be found using our formulas and models, and their LMC parameters. This is even true for the sophisticated N-body calculation of Weinberg (1999); substituting in his final values of parameters gives nearly the same answer as he found from his interacting and tidally disrupted model. We conclude that disagreements about the values of optical depth can be traced to disagreements about parameter choices. Workers with values of optical depth above  $10^{-7}$  all chose parameters outside of our allowed range.

Clearly, to settle these questions, better observations of the stellar components of the LMC and its environs are needed. Direct evidence for a stellar component with an extended or halo geometry would be a key to confirming a non-dark matter explanation for LMC microlensing. We now discuss some of the individual models in more detail.

Aubourg *et al.* (1999) have suggested an LMC model which would produce a self lensing optical depth of  $\sim 1.3 \cdot 10^{-7}$ . If true, this would appear to solve the LMC microlensing problem. Unfortunately, there are serious objections to be raised against the stellar lensing population they employ, since there are

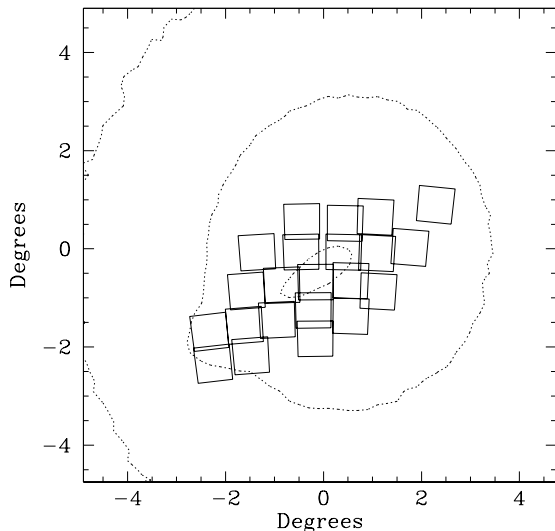


Fig. 7.— Same as figure 6, but for lensing by the LMC halo. Note that the distribution is much less compact than the corresponding disk/bar result; that is, the contours are much more widely spaced out.



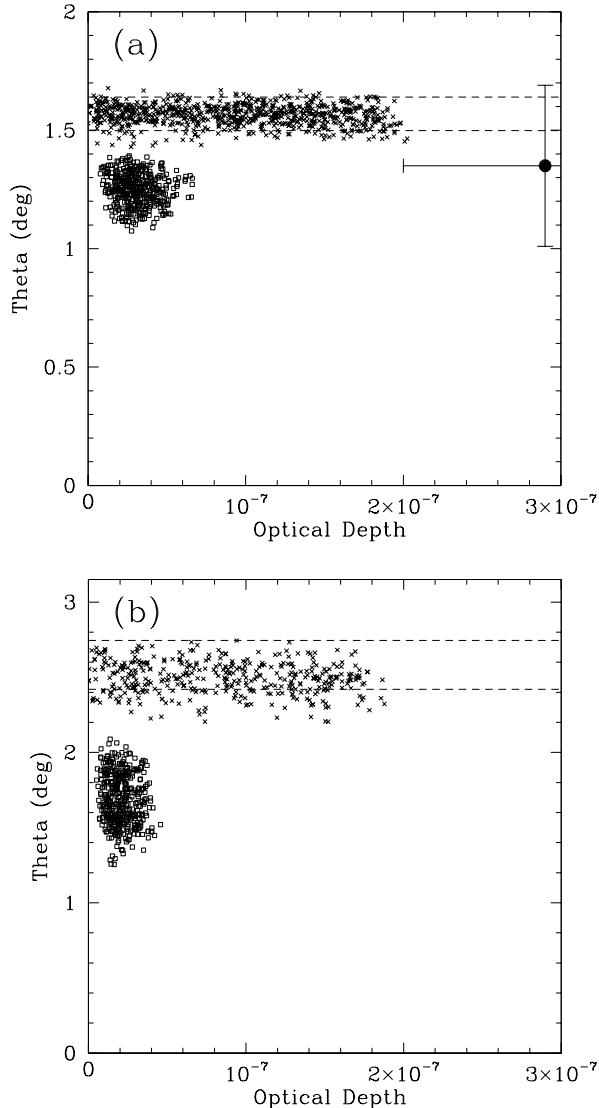


Fig. 8.—  $\tau$  vs.  $\tilde{\theta}$ . Panel (a) shows the range of  $\tau$  and  $\tilde{\theta}$  for the 22 field set, and (b) shows the same for the 82 field set. The open boxes are for the disk/bar, and the x's are for the LMC halo. The points were randomly selected uniformly in parameter space, within the allowed ranges. The dashed lines show the range for MW halo lensing. The point with error bars corresponds to the MACHO year 2 events (Alcock et al. 1997a). Note the increased separation of the disk/bar and halo distributions for the 82 field set.

no known tracer populations. In particular, the lenses in their model, which are ordinary stars, typically have masses between  $0.1-1 M_{\odot}$ , and the vast majority are arranged in a spherical (axis ratio  $\sim 0.9$ ) isothermal distribution with velocity dispersion  $\sim 45$  km/s. This profile and velocity are inconsistent with a multitude of tracers of the old population. Among these are the OLPV results of Bessel et al. (1986) and Hughes et al. (1991), the metal poor giants of Olszewski et al. (1993) and halo-type CH stars of Cowley & Hartwick (1991). While arguments could be made that any individual tracer is not really old or does not represent the old population as a whole, taken together the evidence against the bulk of the mass of the LMC being in the form of an old *stellar* halo is strong. Indeed, the distribution of old clusters (Schommer, et al. 1992) and the RR Lyrae star counts (Alves, et al. 1999) are particularly telling as they are almost certainly an ancient population. The Aubourg et al. model thus appears to be at odds with current observations of the LMC disk. Additionally, it is unclear that the process they invoke for populating their spheroidal component, stochastic heating of the disk by inhomogeneities in the disk itself, would be capable of ejecting upwards of 80% of the LMC disk mass into a far less centrally concentrated pseudosphere.

We can recast their model, however, in a potentially more palatable form. The MACHOs conjectured to reside in the halo of *our* Galaxy have mass of about  $0.2-0.8 M_{\odot}$ , and are modeled in a spherical pseudoisothermal distribution. Note the striking resemblance between the conjectured Milky Way MACHOs and the LMC lenses proposed by Aubourg et al. Whether one chooses to call these undetected objects stars or MACHOs becomes a matter of semantics; we see that the Aubourg et al. model is identical in practice to a MACHO halo around the LMC. As expected, therefore, their results match our calculation for disk-halo lensing.

Very recently, Weinberg (1999b) has suggested that a substantial portion (perhaps all) of the LMC microlensing might be due to LMC disk self lensing. He models the LMC self-consistently with a sophisticated N-body code and finds that the effect of the time-varying Galactic tidal forces is to puff up the LMC disk by a factor ( $\gtrsim 2\times$ ) without noticeably increasing the velocity dispersion. This is important since the optical depth depends strongly on scale height. Indeed, if this simulation does in fact

resemble the LMC's history, then it argues against reliance upon thin-disk equilibrium solutions to the Jeans equations, *a la* Gould (1995). Weinberg's reported optical depth is  $1.4 \cdot 10^{-7}$ , which compares favorably with the recent estimates from the MACHO collaboration ( $\sim 2.0 \cdot 10^{-7}$ ) (Sutherland 1996). A few points need to be made regarding this result. First, this optical depth appears to be calculated for the line of sight to the center of the LMC, instead of averaging over the observational fields. This will yield results biased upward by a factor of about 1.5. Second, Weinberg assumes an inclination of  $45^\circ$ . Using the more likely preferred value of  $30^\circ$ , yields a further 15% reduction (see Weinberg's figure 12). Finally, the disk mass taken in his study,  $10^{10} M_\odot$  appears unrealistically high. As discussed above, (and matching nicely with Weinberg's own calculations in his Appendix A) the *disk* mass is unlikely to be above  $5 \cdot 10^9 M_\odot$ . Taking all of these adjustments into account the optical depth is reduced to  $\sim 4 \cdot 10^{-8}$ , falling in line with the values calculated in this work.

Finally, we should note that Zhao (1998) has suggested that an intervening dwarf galaxy similar to the Sagittarius dwarf could be responsible for the LMC microlensing events. Searches for the RR Lyrae stars that should be contained in such a dwarf turned up negatively (Alcock, et al. 1997b), but Zaritsky & Lin (1997) evaded these search limits by hypothesizing the existence of either a dwarf galaxy very near the LMC itself, or perhaps a tidal tail pulled from the LMC by a close encounter with the SMC. They claimed detection of a population of stars from this intervening entity. This result has been disputed in several ways by several groups. Gould (1998) and Bennett (1998) claim that the optical depth due to the Zaritsky & Lin population is insufficient to explain the microlensing results. Beaulieu & Sackett (1998) claim that the Zaritsky & Lin stars are ordinary LMC stars that are brighter due to stellar evolution, and thus do not represent an intervening population. The discussion continues (Zaritsky, et al. 1999; Gould 1999), and at this point, while the question has not been definitively settled, the case for an intervening dwarf looks rather weak.

## 6. Discussion

We have seen that pure LMC disk/bar self-lensing models appear incapable of producing the measured optical depth of  $\tau \approx 2.9 \cdot 10^{-7}$ . Given the current

state of observations of the LMC, the most likely self-lensing optical depth is an order of magnitude too small to account for the observed events. A reasonable range of self lensing optical depths is  $0.47 - 7.84 \cdot 10^{-8}$  depending upon model parameters. We have shown that halo models can reproduce the optical depth, *if* we are allowed to push the model's parameters to their extremes. We pointed out that numerous observations already limit our ability to push the parameters very far. In order to invoke a self-lensing explanation of LMC microlensing, observation of a sufficient number of stars exhibiting the characteristics of an extended halo seems crucial. Better observations of the LMC that more strongly constrain the disk scale height, inclination, disk mass, total mass, and velocity dispersion also are important as they will reduce the allowed range of optical depth. Especially important are measurements of velocity dispersions and spatial extent of old populations such as RR Lyrae.

We then discussed how consideration of the distribution of optical depth over the face of the LMC can help further distinguish between models. In particular, LMC disk/bar lensing will produce events clustered around the LMC center, while LMC halo lensing will produce a more diffuse distribution of events. We introduced a new clustering statistic, and showed that more microlensing observations distributed over the face of the LMC can be very useful in identifying LMC disk/bar self lensing. However, distinguishing between an LMC halo and the Milky Way halo will probably not be possible using this method.

Finally, we note that if the distance of some of the lenses could be directly determined, the puzzle could be solved. There are several ways to do this using microlensing fine-structure, and the distance to at least one binary SMC lens has been well determined (Alcock, et al. 1998; Afonso, et al. 1998; Albrow, et al. 1998). One LMC binary lens (LMC-9) for which such a determination was possible was unfortunately not sampled well enough to allow a secure distance determination (Bennett, et al. 1996), but continued monitoring should eventually allow some distances to be found. Perhaps the most secure distance determination would come from astrometric parallax effects in microlensing. NASA's Space Interferometry Mission (SIM), scheduled for launch about 2005, should have the astrometric resolution to make definitive parallax measurements (Paczynski 1998; Boden et al. 1998).

It has been argued that the SMC events along

with LMC-9 strongly support the notion that all of the events are due to self-lensing. In this view, the next LMC binary event should definitively decide between halo and self lensing scenarios. This may not be the case. First, the SMC is *expected* to have a high self-lensing rate regardless of the nature of the LMC lenses. Coupled with the uncertain interpretation of LMC-9, the case for LMC self lensing is poorly supported at present. In this light, the next LMC binary event alone will probably not suffice to locate the bulk of the lenses, even if it is found to be an LMC lens. First, we've seen that LMC self lensing may well contribute of order 10-20% of the lensing, so that some self-lensing events are expected. Secondly, there may well be fewer binaries in the Halo than the LMC, inducing a possible selection effect in favor of LMC lenses. It will probably require multiple future distance determinations to settle this matter.

Given the importance of the LMC microlensing interpretation to the dark matter question, many of the potential observational efforts described above are being attempted. We are hopeful that the interpretation of LMC microlensing will become clear within the next few years.

### Acknowledgements

It is a pleasure to thank Thor Vandehei for numerous enlightening and stimulating discussions on this and related matters. We acknowledge support from the U.S. Department of Energy, under grant DEFG0390ER 40546, and from Research Corporation under a Cottrell Scholar award.

### REFERENCES

Afonso, C., et al. 1998, A&A, 337, L17  
 Albrow, M., et al. 1998, ApJ submitted, preprint astro-ph/9807086  
 Alcock, C., et al. 1997, ApJ, 486, 697  
 Alcock, C., et al. 1997, 490, L59  
 Alcock, C., et al. 1997, ApJ, 491, L11  
 Alcock, C., et al. 1998, ApJ submitted, preprint astro-ph/9807163  
 Alves, D. 1998, PhD thesis, University of California, Davis

Aubourg, E., et al. 1999, A&A submitted, preprint astro-ph/9901372  
 Bahcall, J. & Tremaine, S. 1981, ApJ, 244, 805  
 Beaulieu, J. & Sackett, P. 1998, AJ, 116, 209  
 Bennett, D. 1998, 493, L79  
 Bennett, D., et al. 1996, Nucl. Phys. Proc. Suppl., 51B, 152-156  
 Bessel, M.S., Freeman, K.C., & Wood, P.R., 1986, ApJ, 310, 710  
 Binney, J. & Tremaine, S., 1987, "Galactic Dynamics", Princeton University Press  
 Blackman, C. P. 1983, MNRAS, 202, 379  
 Boden, A., Shao, M. & Van Buren, D. 1998, ApJ, 502, 538  
 Bothun, G. D. & Thompson, I. B. 1988, AJ, 96, 877  
 Caldwell, J.A.R. & Coulson, I.M. 1986, MNRAS 218, 223  
 Carignan, C. & Purton, C. 1998, ApJ, 506, 125  
 Cowley & Hartwick, 1991, ApJ, 373, 80  
 de Vaucouleurs, G. 1957, AJ, 62, 69  
 Dottori, H., et al. 1996, ApJ, 461, 742  
 Dwek, et al. 1995, ApJ, 445, 716  
 Fields, B.D., Freese, K. & Graff, D.S., 1998, New Astronomy 3, 347  
 Freeman, K. C. 1996, in Buta, R., Crocker, D. A., & Elmegreen, B. G. eds., 1996, "Barred Galaxies", PASP, 91, p. 1  
 Gates, E., Gyuk, G., & Turner, M. 1996, PRD, 53, 4138  
 Gould, A. 1995, ApJ 441, 77  
 Gould, A. 1998, ApJ 499, 728  
 Gould, A. 1999, ApJ submitted, preprint astro-ph/9902374  
 Gould, A., Bahcall, J., & Flynn, C. 1997, ApJ, 482, 913

- Ho, L. C., Filippenko, A. V., & Sargent, W. 1996, in Buta, R., Crocker, D. A., & Elmegreen, B. G. eds., 1996, "Barred Galaxies", PASP, 91, p. 188
- Hughes, S.M.G., Wood, P.R. & Reid, N., 1991, AJ, 101, 1304
- Kenney, J. 1996, in Buta, R., Crocker, D. A., & Elmegreen, B. G. eds., 1996, "Barred Galaxies", PASP, 91, p. 150
- Kerins, E. & Evans, N. W. 1999, ApJ, 517, 734
- Kim, S. et al., 1998, ApJ, 503 674
- Kinman et al., 1991, PASP, 103 1279
- Kunkel, W.E., Demers, S., Irwin, M.J., & Albert, L., 1997, ApJ, 488, L129
- Meatheringham, S.J., Dopita, M.A., Ford, H.C., & Webster, B.L., 1988, ApJ, 327, 651
- Odehahn, S. C. 1996, in Buta, R., Crocker, D. A., & Elmegreen, B. G. eds., 1996, "Barred Galaxies", PASP, 91, p. 30
- Ohta, K. 1996, in Buta, R., Crocker, D. A., & Elmegreen, B. G. eds., 1996, "Barred Galaxies", PASP, 91, p. 37
- Oestreicher, M., & Schmidt-Kaler, T. 1996, A&AS, 117, 303
- Olszewski, E. W. 1993, in Smith, G. & Brodie, J., eds. 1993, ASP Conf. Ser. 48, p. 351
- Olszewski, E.W., Suntzeff, N.B., & Mateo, M., 1996, ARA&A, 34, 511
- Paczynski, B. 1998, ApJ 494, L23
- Palanque-Delabrouille, N., et al. 1998, A&A, 332, 1
- Prevot, L., Rousseau, J. & Martin, N., 1989, A&A, 225, 303
- Sahu, K.C. 1994, Nature, 370, 275
- Sahu, K.C. 1994, PASP, 106, 942
- Sahu, K.C. & Sahu, M. S. 1998, ApJ, 508, L147
- Sakamoto, K., et al. 1999, ApJ in press, preprint astro-ph/9906454
- Salati, P., et al. 1999, A&A submitted, preprint astro-ph/9904400
- Schommer, R.A., Olszewski, E.W, Suntzeff, N.B. & Harris, H.C., 1992, AJ 103, 447
- Sutherland, W. 1996, astro-ph/9611059
- Udalski, A., Kubiak, M., Szymanski, M., 1997, Acta Astronomica, 47, 319
- Weinberg, M. 1998, ApJ submitted, preprint astro-ph/9811204
- Weinberg, M. 1999, ApJ submitted, preprint astro-ph/9905305
- Weiner, B. & Sellwood, J. 1999, ApJ submitted, preprint astro-ph/9904130
- Welch, D.L., *et al.* 1987, ApJ 321, 162
- Westerlund, B. 1997, "The Magellanic Clouds". Cambridge University Press: Cambridge, UK.
- Vandehai, T. 1998, poster at AAS meeting 192, Washington D.C.
- Yamashita, Y. 1975, PASJ, 27, 325
- Zaritsky, D. & Lin, D.N.C., 1997, AJ, 114, 2545
- Zaritsky, D., Shectman, S., Thompson, I., Harris, J. & Lin, D.N.C., 1999, AJ, 117, 2268
- Zhao, H., 1998, MNRAS, 294, 139